Chandra Telescope Optical Axis and Aimpoint

Ping Zhao

Chandra X-ray Center
Smithsonian Astrophysical Observatory
60 Garden Street, Cambridge, MA 02138

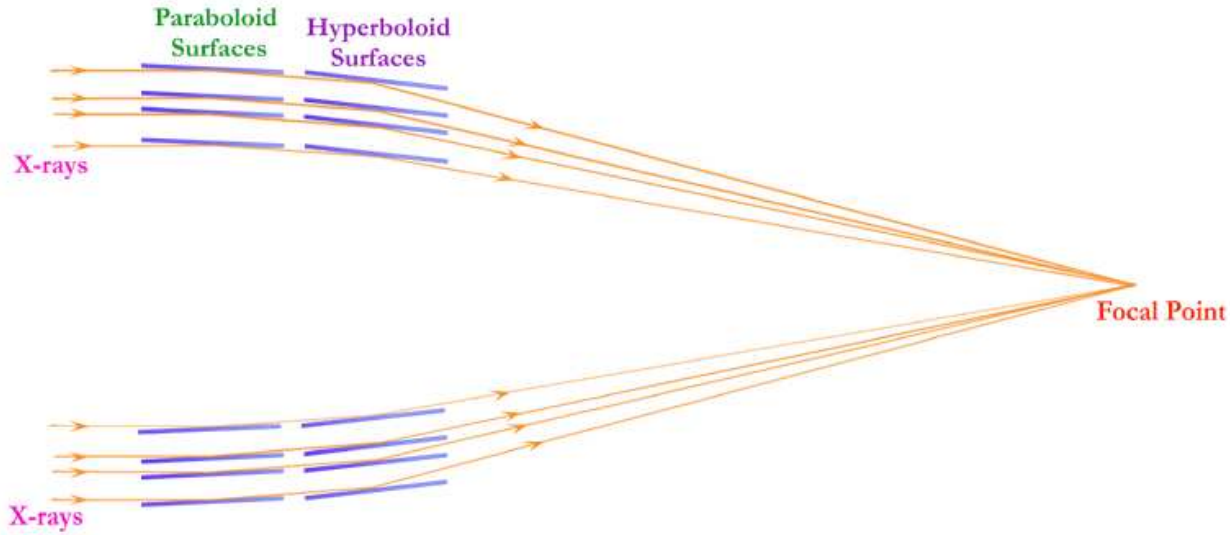

Optical Axis, Focal Point and Aimpoint

The positions of the Optical Axis, Focal Point and Aimpoint are critical for the optimal operation of the Chandra X-ray Observatory.

Definition:

- **Focal Point: Point on the focal plane where the sharpest PSF is located.**
- **Optical Axis: Axis that perpendicular to the focal plane at the Focal Point.**
- **Aimpoint: Point on the focal plane where the image of a source with zero Y and Z offsets is located.**

For an ideal Wolter-I Mirror:

- **Optical Axis is the mathematical axis of both paraboloid and hyperboloid mirror surfaces; and it passes through both Focal Point and Aimpoint (i.e. Focal Point and Aimpoint is the same point).**

For the actual HRMA:

- **The Focal point and the Aimpoint were not at the same point**
- **The positions of the Optical Axis and Aimpoint have been monitored continuously.**
- **Both the Optical Axis and the Aimpoint have been drifting since the Chandra launch.**

Questions:

- **How much and and how fast have they been drifting?**
- **How do their drifts affect the Chandra operation?**

SIM Translation Table

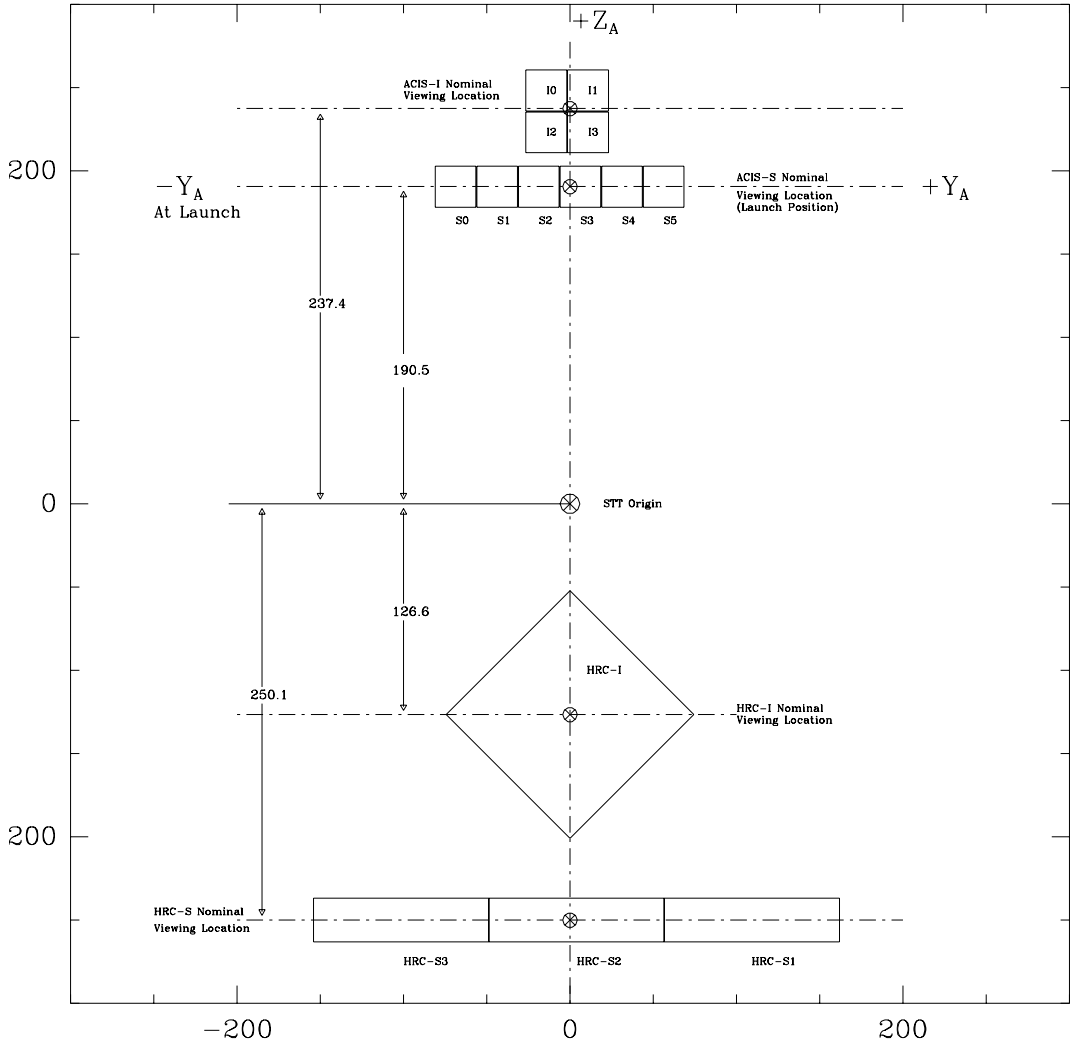

Figure 1: The Chandra Science Instrument Module (SIM) Translation Table, showing the flight focal plane instrument to scale. Distance in mm. Coordinate system is AXAF-STT-1.0.

On-orbit calibration of the Optical Axis

The HRC-I and HRC-S gain maps were calibrated by using raster scans of Y and Z offset with bright point sources (HR 1099 and Ar Lac). These calibration data are used to determine the position of the Chandra Optical Axis.

Optical Axis Calibration data (until Sept. 2007)

Detector: HRC-I

Date	Source	Sim-Z (mm)
1999-09-02	HR 1099	91.8655
1999-10-03	Ar Lac	126.9855
1999-12-09	Ar Lac	126.9855
2000-12-12	Ar Lac	126.9855
2002-01-26	Ar Lac	126.9855
2003-02-22	Ar Lac	126.9855
2004-11-25	Ar Lac	126.9855
2005-09-27	Ar Lac	126.9830
2006-09-20	Ar Lac	126.9830
2007-09-17	Ar Lac	126.9855

Detector: HRC-S

Date	Source	Sim-Z (mm)
2000-12-20	Ar Lac	250.4660
2001-05-14	Ar Lac	250.4660
2002-01-26	Ar Lac	250.4660
2002-08-09	Ar Lac	250.4660
2003-02-22	Ar Lac	250.4660
2003-09-01	Ar Lac	250.4660
2004-02-09	Ar Lac	250.4660
2004-11-28	Ar Lac	250.4660
2005-02-10	Ar Lac	250.4660
2005-09-01	Ar Lac	250.4660
2006-03-20	Ar Lac	250.4660
2006-09-21	Ar Lac	250.4660
2007-09-21	Ar Lac	250.4660

Data Analysis

- **Encircled energy radii (10% – 99%) of each raster scan images (in sky coordinate) were calculated.**
- **The centroids of ChipX and ChipY were calculated for each point.**
- **The EE radii vs. (ChipX, ChipY) was fit to a quadratic function:**

$$r_{EE_i}(x, y) = c_0 + c_1 x + c_2 y + c_{11} x^2 + c_{12} xy + c_{22} y^2 \quad (1)$$

  where i = 10% – 99%.
- **By definition, optical axis is located at (x_0, y_0) where r_{EE_i} reaches minimum.**
- **Aimpoint positions were calculated for each set of raster scan, using the script provided by Jonathan McDowell.**

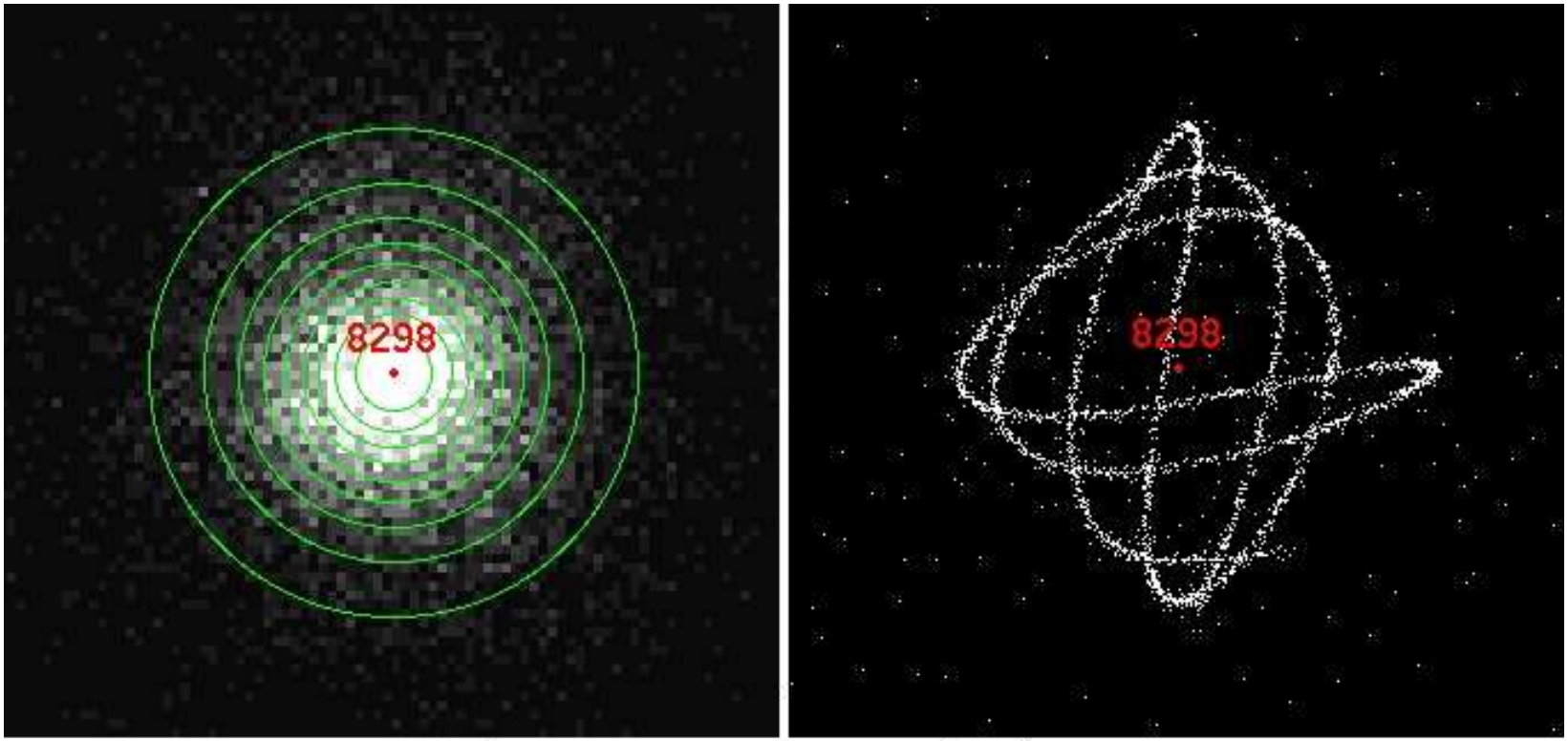

Figure 2: HRC-I observation of Ar Lac with 3ks exposure time and zero Y and Z offsets (obsid 8298, observed Sept. 2007). Left: image in sky coordinates with the centroid marked and 10% – 90% encircled energy circle overlay; Right: image in chip coordinates with the centroid of the Lissajous dither pattern (40″ peak-to peak) marked.

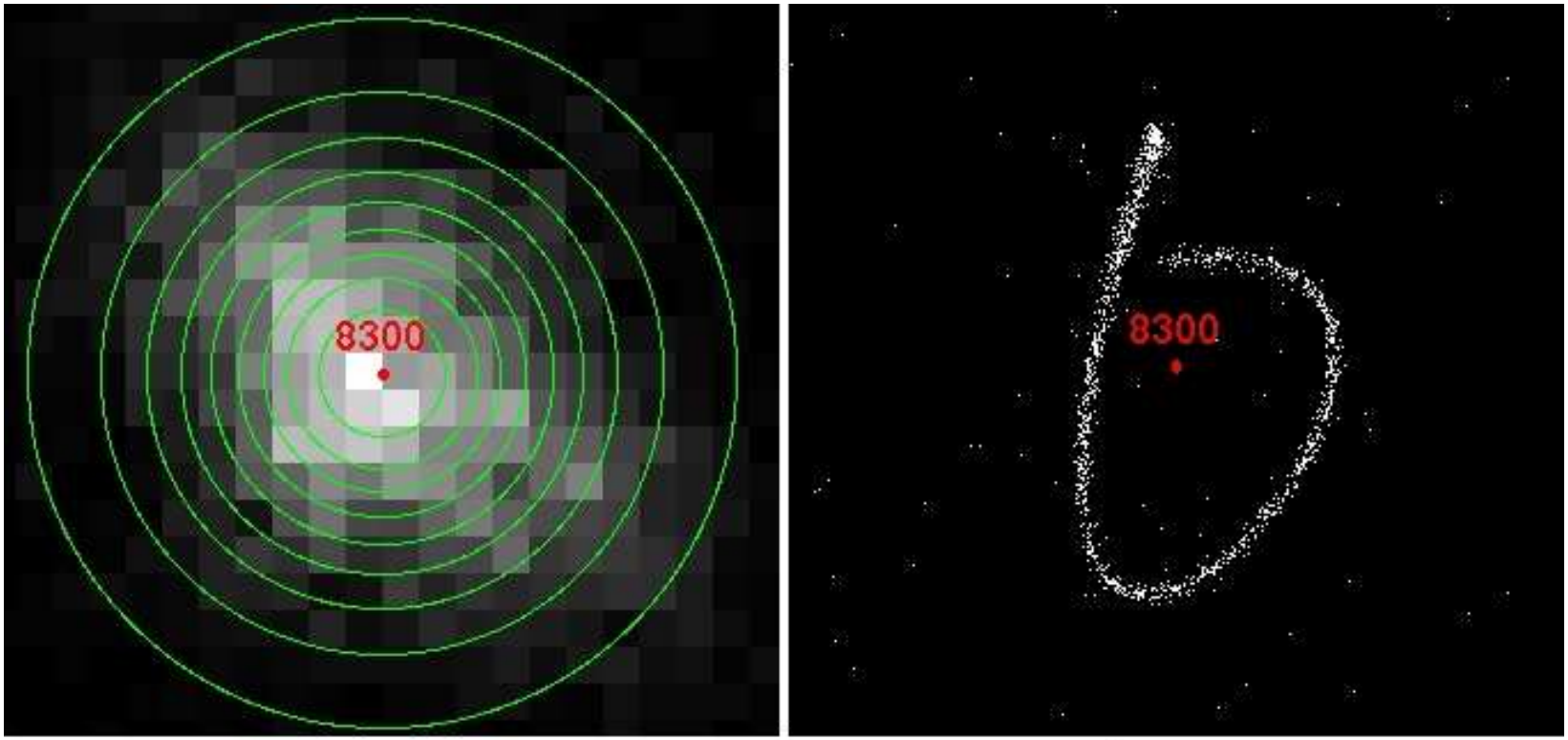

Figure 3: HRC-I observation of Ar Lac with 1ks exposure time and Y-offset=0 and Z-offsets=2 arcmin (obsid 8300, observed Sept. 2007). Left: image in sky coordinates with the centroid marked and 10% – 90% encircled energy circle overlay; Right: image in chip coordinates with the centroid of the Lissajous dither pattern (40″ peak-to peak) marked.

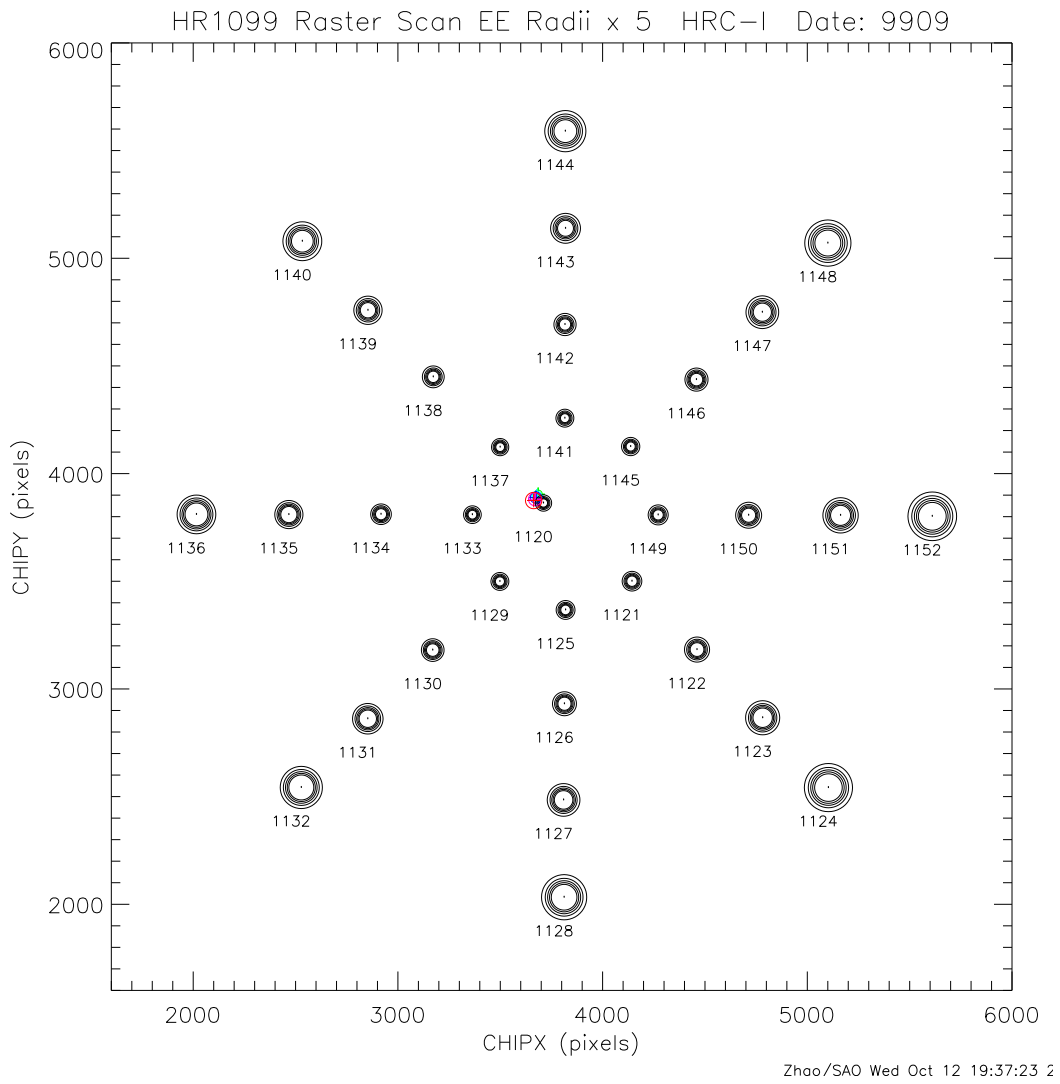

Figure 4: HRC-I raster scan of HR 1099 with 1ks exposure time for each point (Date: 1999-09-02). Circles around each observation point are the 50%–90% EE circles × 5.

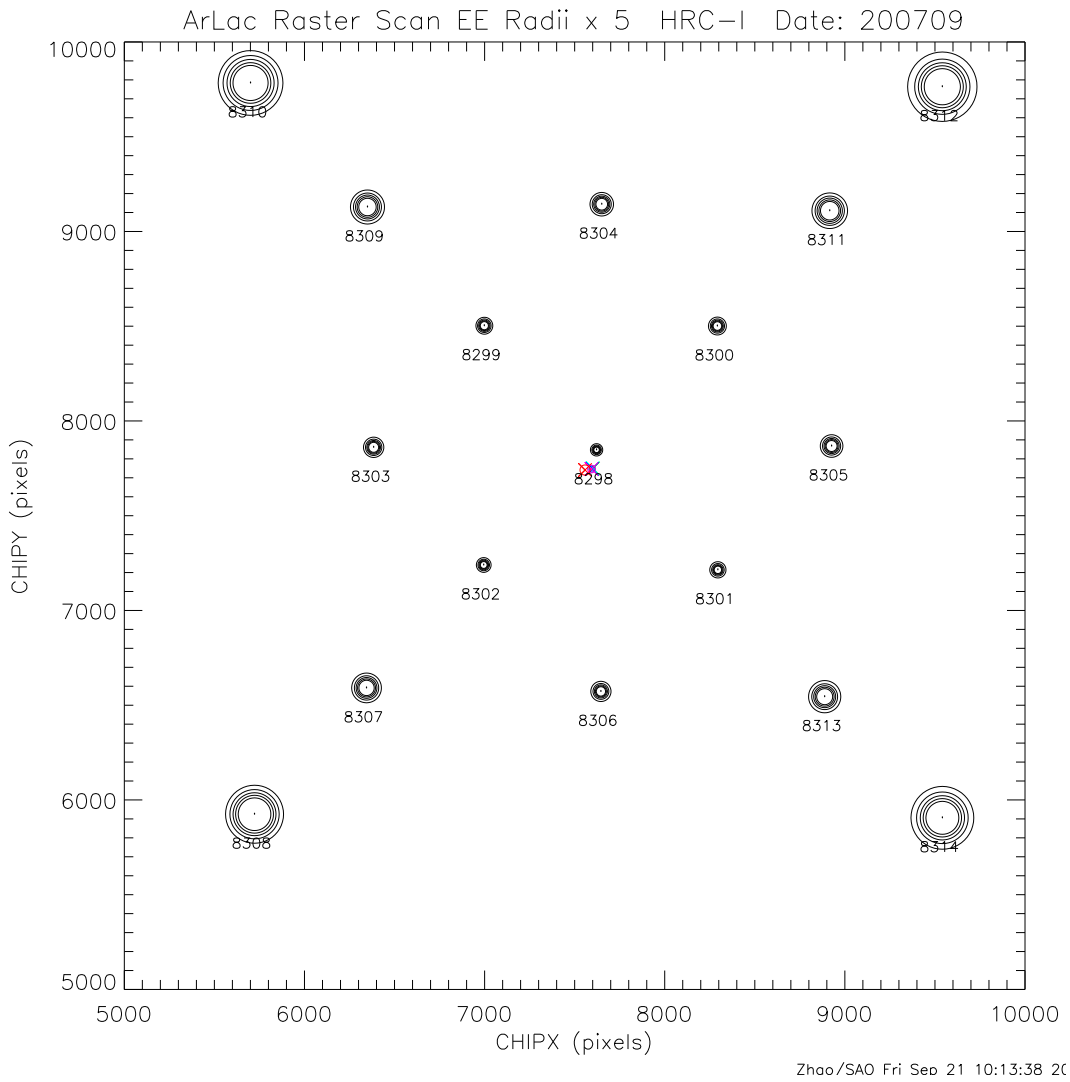

Figure 5: HRC-I raster scan of Ar Lac with 1ks exposure time for each point, except the center point which is 3ks (Date: 2007-09-17). Circles around each observation point are the 50% − 90% EE circles × 5.

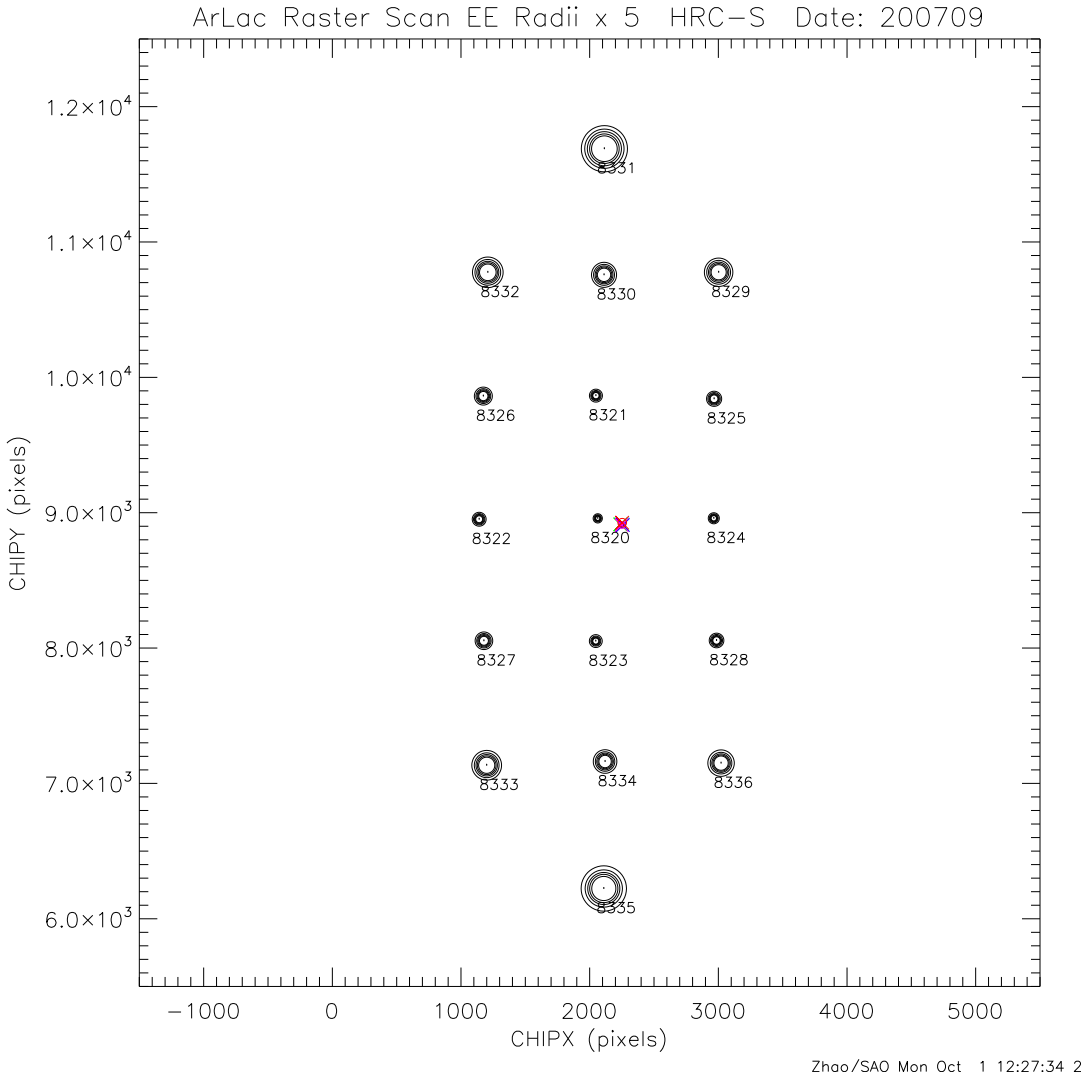

Figure 6: HRC-S raster scan of Ar Lac with 1ks exposure time for each point, except the center point which is 3ks (Date: 2007-09-21). Circles around each observation point are the 50% − 90% EE circles × 5.

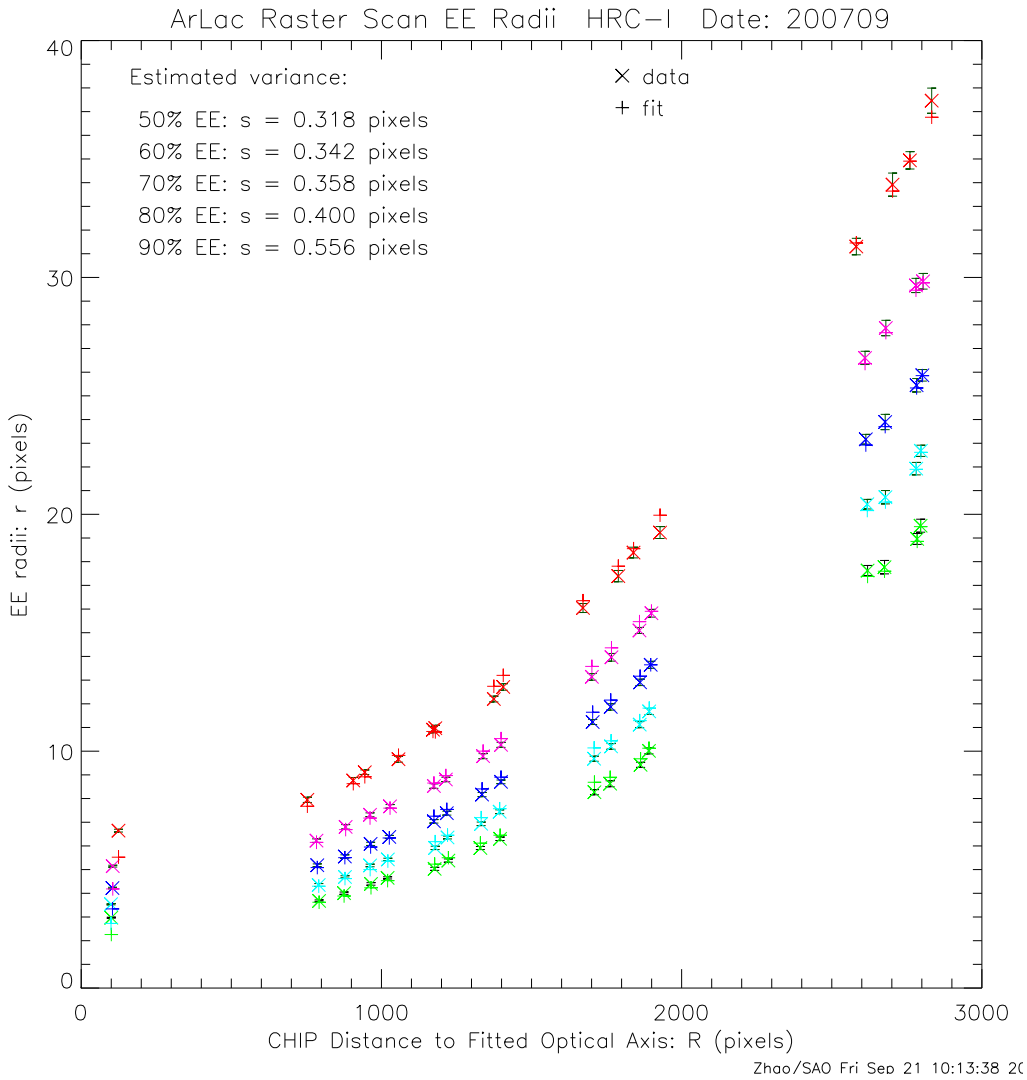

Figure 7: Quadratic fit of HRC-I raster scan data of Ar Lac (Date: 2007-09-17).

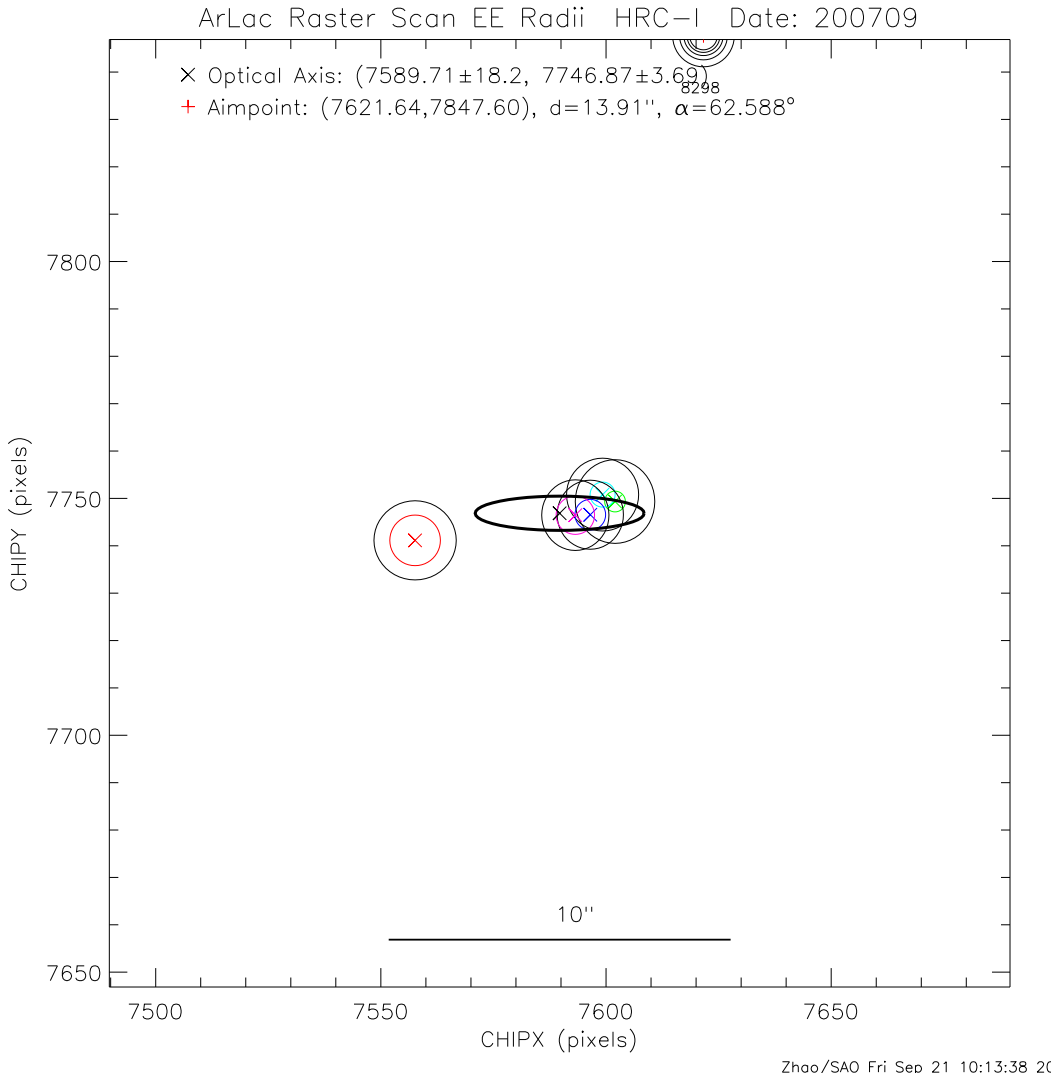

Figure 8: Optical Axis and Aimpoint position on HRC-I, based on raster scan observation of Ar Lac made on 2005-09-17. The Optical Axis is the weighted average of five EE (50% – 90%) measurements, at the center of the error ellipse. The Aimpoint (the center point with the zero Y and Z offsets) is at the upper border. The two points are 13.91″ apart.

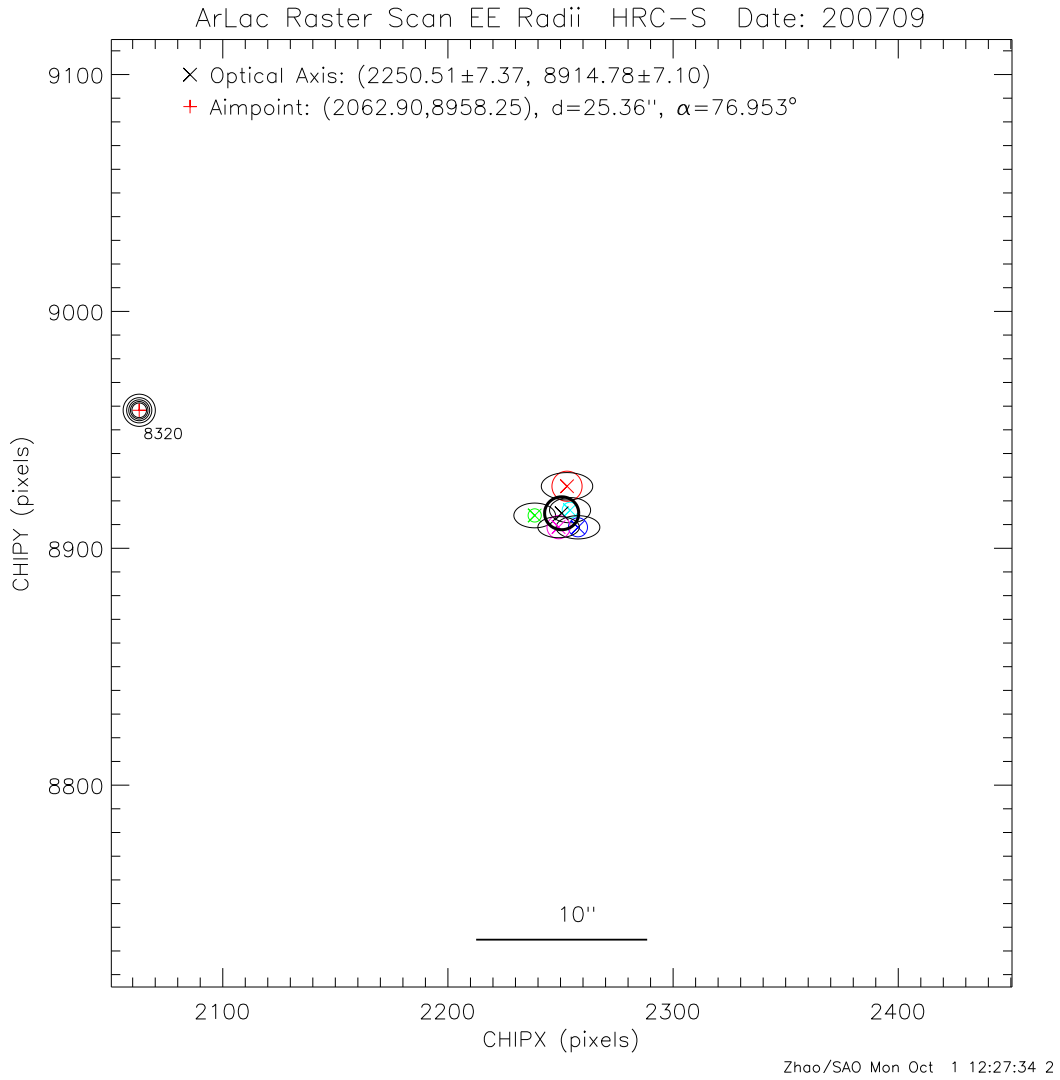

Figure 9: Optical Axis and Aimpoint position on HRC-S, based on raster scan observation of Ar Lac made on 2005-09-21. The Optical Axis is the weighted average of five EE (50% – 90%) measurements, at the center of the error ellipse. The Aimpoint (the center point with the zero Y and Z offsets) is near the left border. The two points are 25.36″ apart.

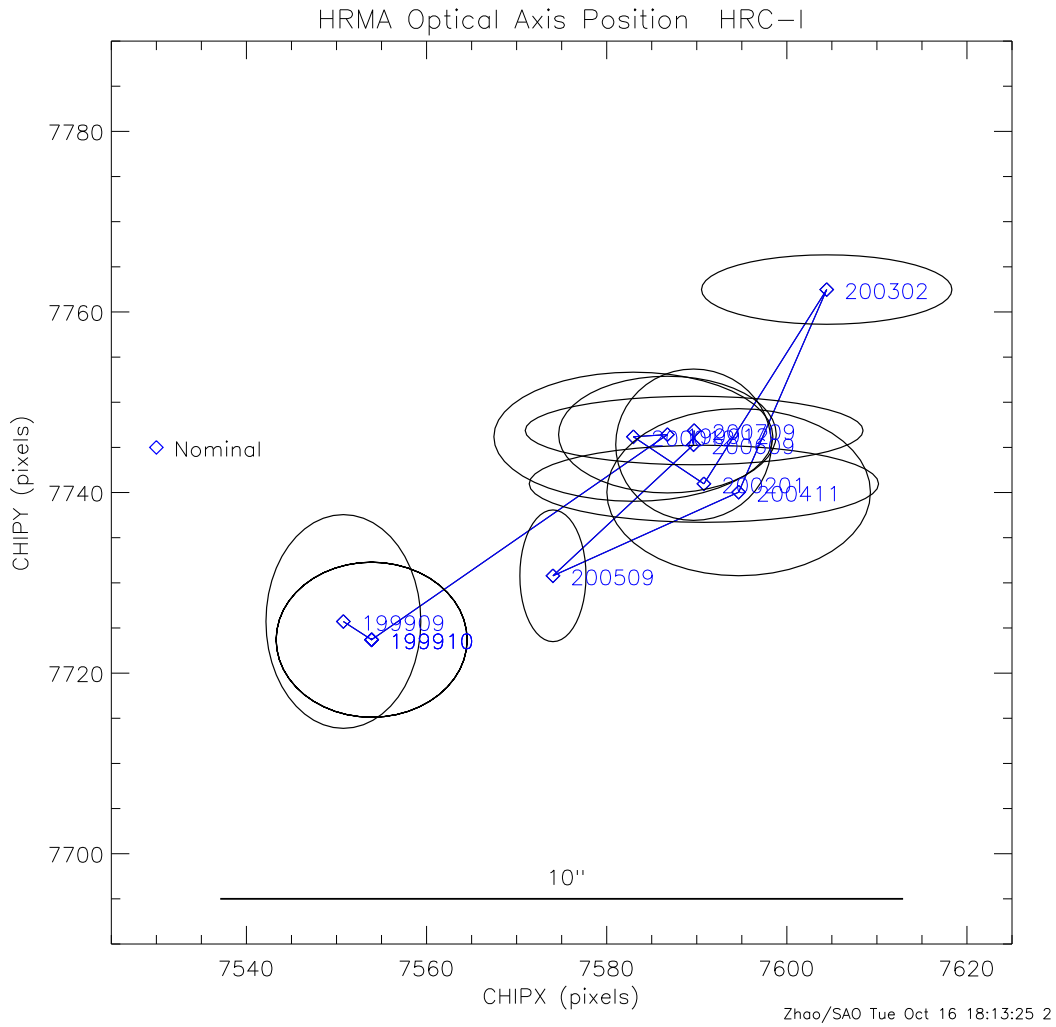

Figure 10: Optical Axis positions from all the HRC-I measurements on CHIP coordinates. The drift of the Optical Axis is more like a random walk within 10″.

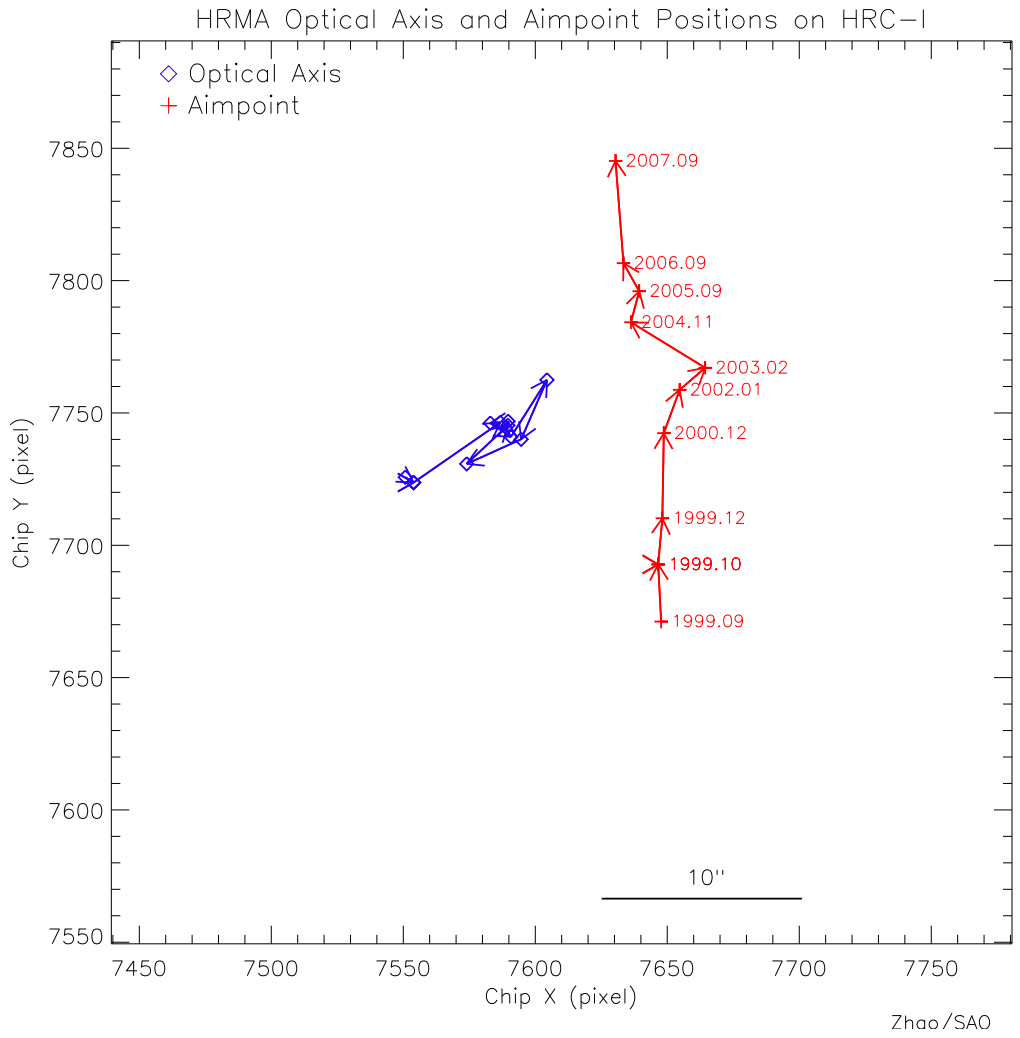

Figure 11: Optical Axis and Aimpoint positions from all the HRC-I measurements on CHIP coordinates. The Aimpoint has drifted by more than 24″ in the -Y and -Z direction of the SIM coordinates. But the two points were never 15″ apart.

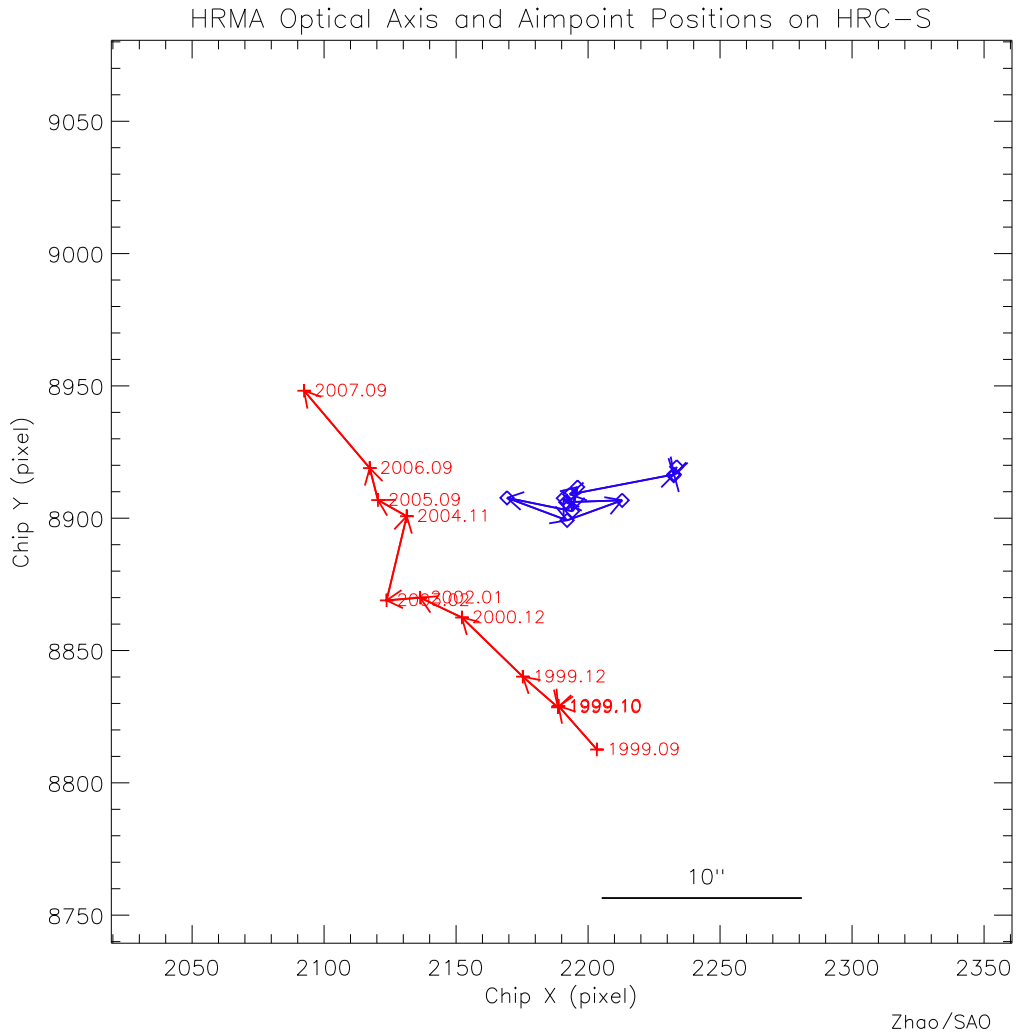

Figure 12: Chandra Optical Axis and Aimpoint positions on HRC-S, transformed from the HRC-I measurements.

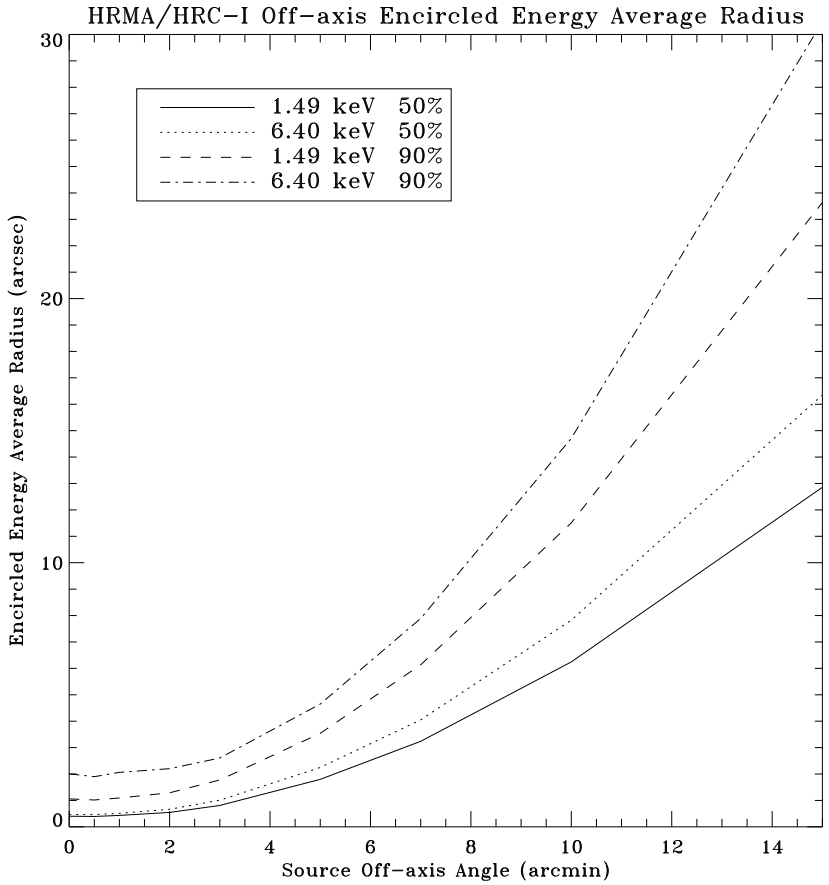

Figure 4.11: **HRMA**/HRC-I encircled energy average radii for circles enclosing 50% and 90% of the power at 1.49 and 6.40 keV as a function of off-axis angle. The HRC-I surface is a flat plane perpendicular to the optical axis, which does not follow the curved *Chandra* focal plane. These curves include the blurs due to the HRC-I spatial resolution and the *Chandra* aspect error.

Figure 13: The HRMA/HRC-I Encircled Energy as a function of off-axis angle (POG: Figure 4.11). It shows that the current small separation ($< 15''$) between the Optical Axis and the Aimpoint does not degrade the onaxis target PSF on the HRC.

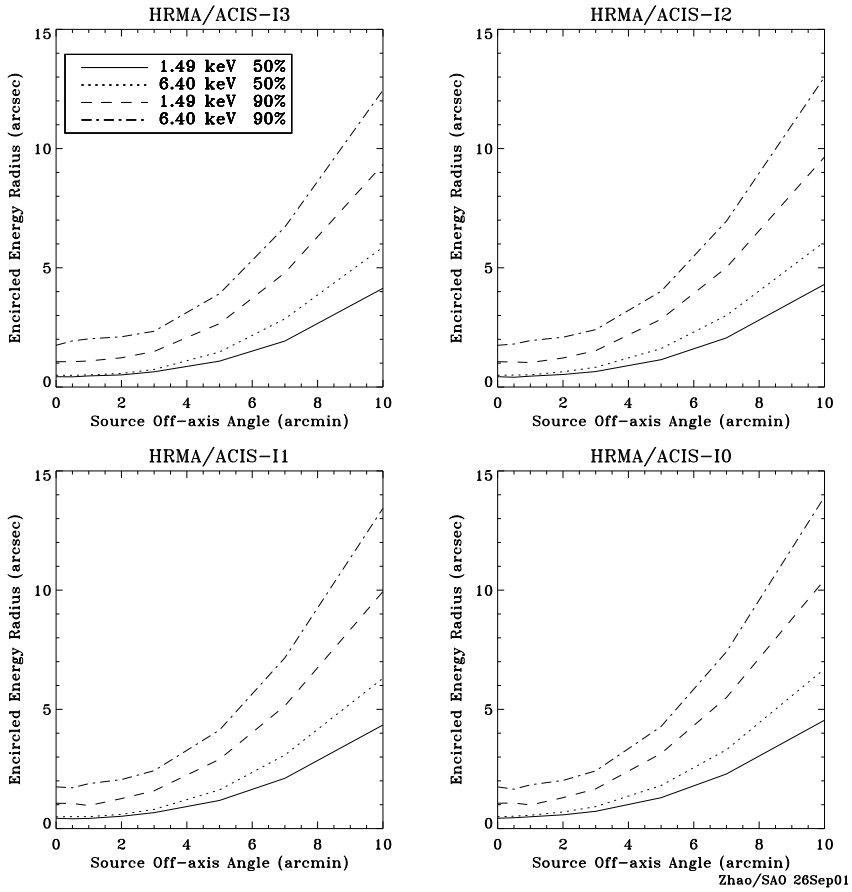

Figure 4.12: **HRMA**/ACIS-I encircled energy radii for circles enclosing 50% and 90% of the power at 1.49 and 6.40 keV as a function of off-axis angle. The ACIS-I surface is composed by four tilted flat chips which approximate the curved *Chandra* focal plane. The HRMA optical axis passes near the aimpoint which is located at the inner corner of chip I3. Thus the off-axis encircled energy radii are not azimuthally symmetric. The four panels show these radii's radial dependence in four azimuthal directions – from the aimpoint to the outer corners of the four ACIS-I chips. These curves include the blurs due to the ACIS-I spatial resolution and the *Chandra* aspect error.

Figure 14: The HRMA/ACIS-I Encircled Energy as a function of off-axis angle (POG: Figure 4.11). It shows that the current small separation ($< 15''$) between the Optical Axis and the Aimpoint does not degrade the onaxis target PSF on the ACIS.

ACIS FLIGHT FOCAL PLANE

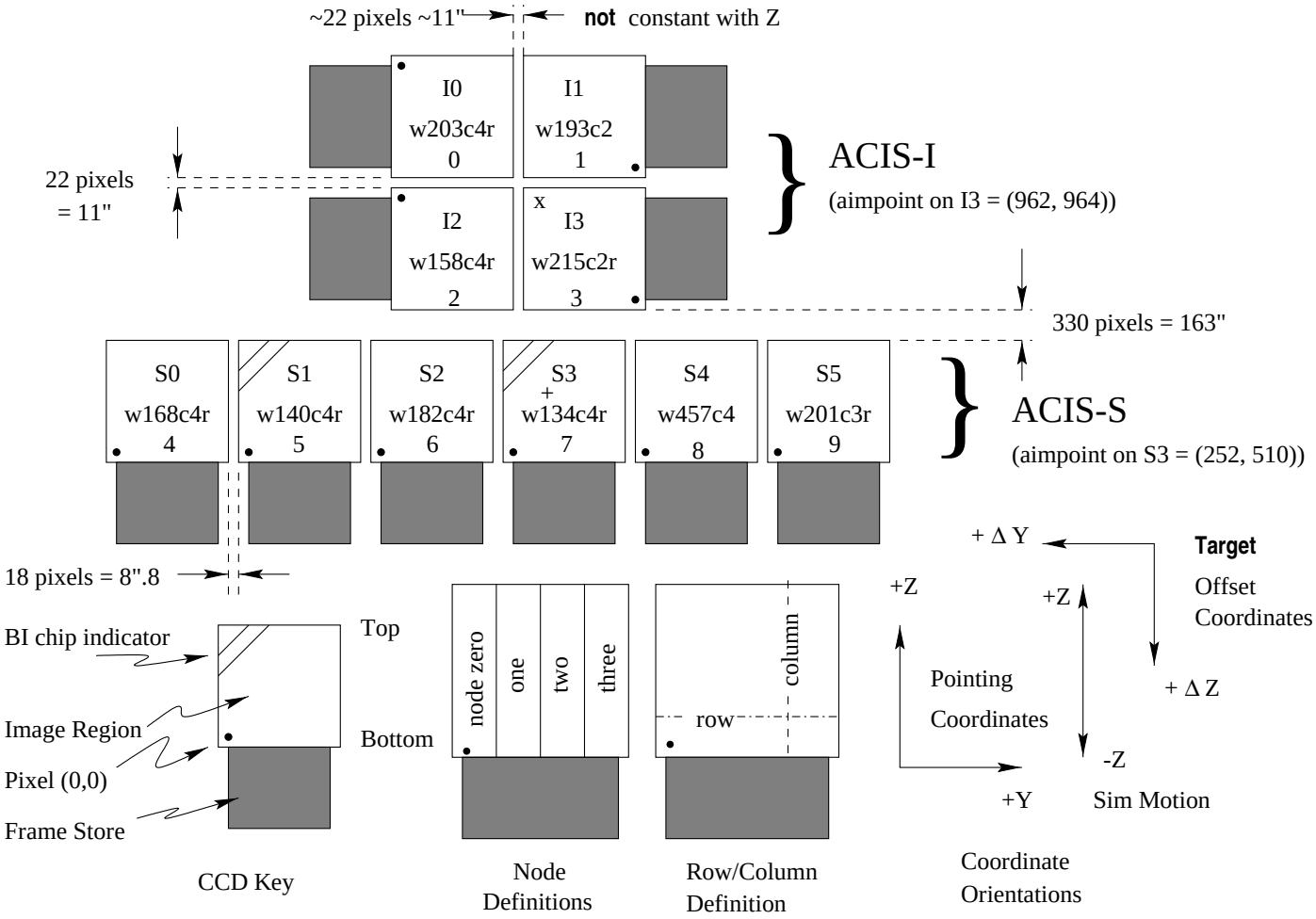

Figure 15: The ACIS focal plane layout (POG: Figure 6.1).

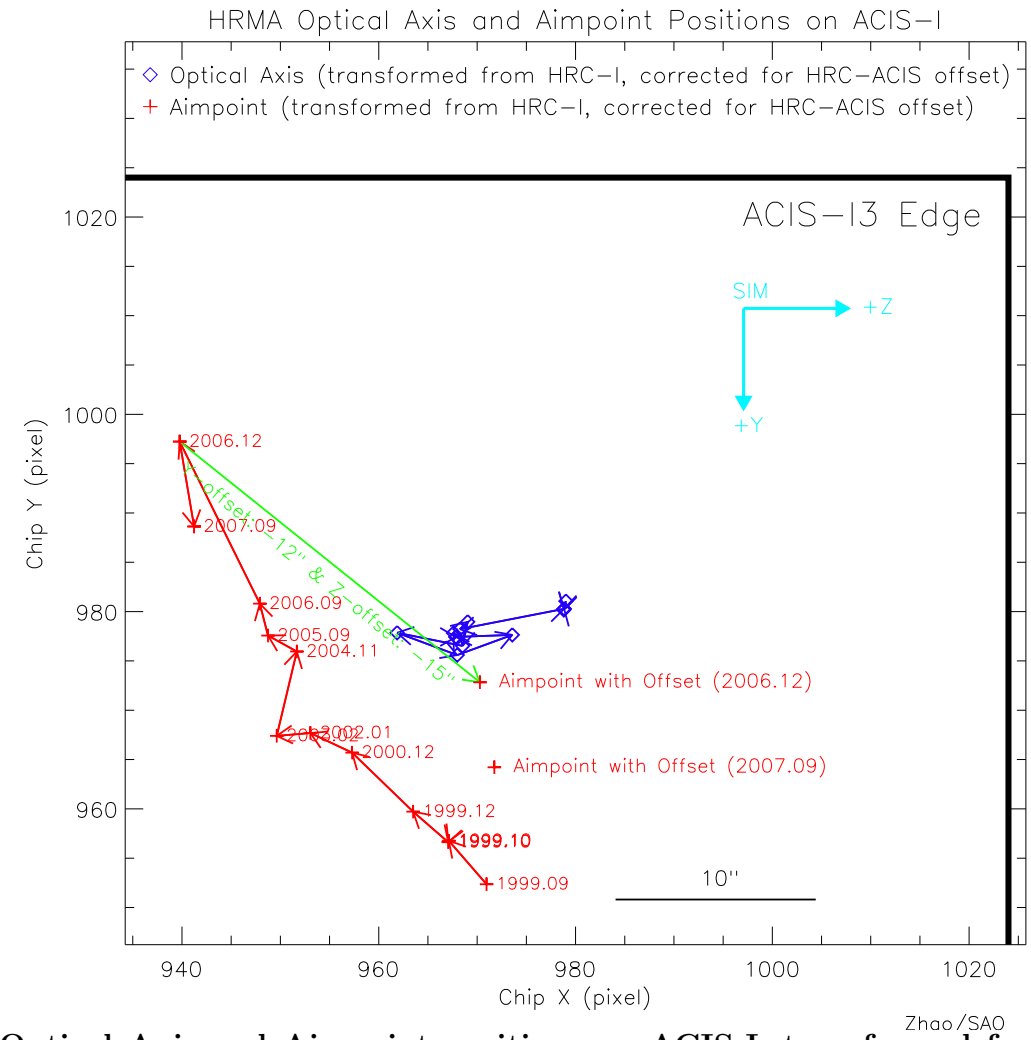

Figure 16: Chandra Optical Axis and Aimpoint positions on ACIS-I, transformed from the HRC-I measurements. A large shift of $\sim 10''$ in December 2006 was caused by the Aspect Camera Assembly (ACA) primary focal plan CCD cool down from $-15°$C to $-20°$C. This sudden shift brought the aimpoint very close to the ACIS-I3 chip boundary. As it continue to drift towards the boundary, the dither pattern ($16''$ peak-to-peak) will soon fall out of the chip. Therefore a default target pointing of Y-offset $= -15''$ and Z-offset $= -12''$ was implemented to bring the aimpoint away from the chip boundary and also closer to the optical axis. Later when the ACA warmed up, the aimpoint drifted back $\sim 4''$. The light blue arrows show the SIM directions.

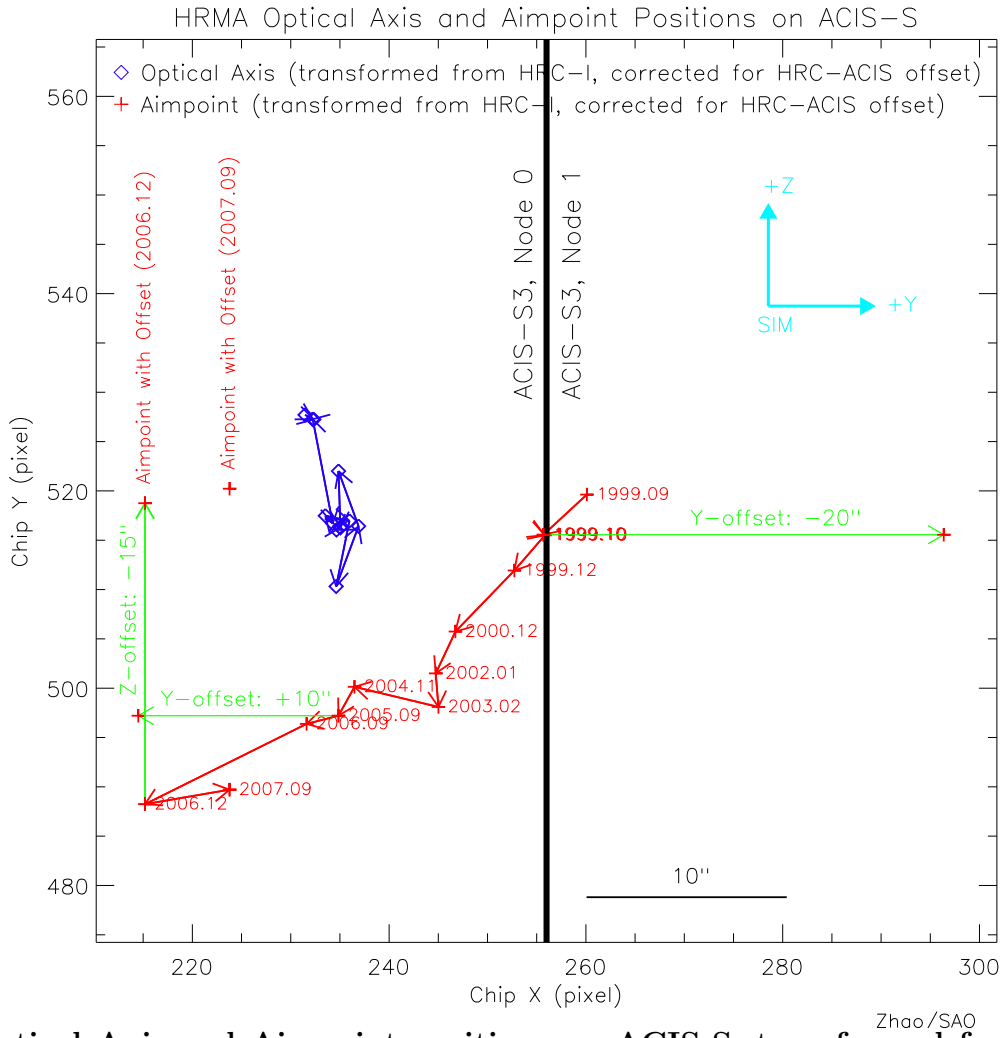

Figure 17: Chandra Optical Axis and Aimpoint positions on ACIS-S, transformed from the HRC-I measurements. Because of the aimpoint drift, the default target pointing offset for ACIS-S observations has been implemented three times to avoid the dither pattern falls on the node boundary: 1) Y-offset=$-20''$ in Oct. 1999; 2) Y-offset=$+10''$ in Sept. 2005; and 3) Z-offset=$-15''$ in Jan. 2007. The last one is to put the target pointing closer to the Optical Axis. The light blue arrows show the SIM directions.

Conclusion

- Since the Chandra launch, its optical axis and aimpoint have been drifting continuously.
- The drift of the optical axis is more like a random walk within 10″ range.
- The Aimpoint has been drifting in the -Y and -Z direction of the SIM coordinates by more than 24″ .
- The relatively small and random drift of the optical axis indicates that the optical bench (connection the HRMA and SIM) and SIM itself are relatively stable.
- The consistent directional drift of the aimpoint indicates that relative alignment between the aspect system and the telescope has been changing constantly in one direction. This is especially true when there is a sudden change in the ASA system such as the cool down.
- The optical axis and the aimpoint were never more than 15″ apart anytime during the Chandra operation. This small separation causes no degradation on the PSF of the on-axis targets.
- The drifts cause no impact for the HRC-I and HRC-S operations.
- The drift of the aimpoint causes the change of the default offset for the on-axis target pointing on both ACIS-S and ACIS-I, to avoid the dither falling on the node boundary or off the chip.
- To monitor the Optical Axis and Aimpoint continuously is essential to ensure the optimal operation of the Chandra X-ray Observatory – THAT IS WHAT WE WILL DO!